Available online at www.sciencedirect.com
ScienceDirect
Nuclear Instruments and Methods in Physics Research B 260 (2007) 628–632
NIM B
Beam Interactions with Materials & Atoms
www.elsevier.com/locate/nimb

Scanning X-ray microfluorescence in a SEM for the analysis of very thin overlayers

E.S. Valamontes [a,b,*], J.C. Statharas [c], C. Nomicos [b]

[a] Department of Telecommunications, University of Peloponnese, GR-22100 Tripoli, Greece
[b] Department of Electronics, Technological and Educational Institute of Athens, 12210 Aegaleo, Greece
[c] Department of Aircraft Technology, Technological and Educational Institute of Chalkis, 34400 Psahna, Euboea, Greece

Received 10 January 2007; received in revised form 24 March 2007
Available online 7 April 2007

Abstract

In this paper, we used back-foil scanning X-ray microfluorescence (SXRF) and we examined the sensitivity of the technique for the analysis of very thin overlayers, where electron probe X-ray microanalysis (EPMA) reaches its detection limits. The lateral resolution of back-foil SXRF is also calculated for all the systems used. Both experimental results and Monte-Carlo calculations are used in this respect. Back-foil SXRF used in optimized experimental conditions, is found to be more sensitive than EPMA, especially in the case of very thin overlayers. The lateral resolution of back-foil SXRF is of the order of some micrometers. This is much better than the lateral resolution in conventional XRF and of the same order of magnitude as in EPMA.

Keywords: X-ray microanalysis; X-ray microfluorescence; Thin films

1. Introduction

X-ray fluorescence (XRF) and X-ray microanalysis (EPMA) are two analytical techniques with quite different characteristics. EPMA uses electron excitation in an electron microscope while XRF uses an X-ray excitation source, which offers several advantages over the electron excitation: (a) more sensitive than energy dispersive EPMA, (b) possibility of analyzing insulators without depositing a conducting layer on the top of them, (c) possibility of nondestructive analysis of beam sensitive biological samples where these are not sensitive to the level of X-radiation involved. On the other hand, EPMA offers the advantage of a much better lateral resolution, in the μm range, which allows imaging of the analyzed element of the sample.

Several attempts have been made to use the electron source of the electron microscope in order to obtain an X-ray source inside the microscope. Middleman and Geller [1] fixed an attachment with a 25 μm thick molybdenum foil, used as an X-ray source, generated by a 30 keV electron beam. Analogous attachments were proposed by Linnemann and Reimer [2], Wendt [3,4] and Weiss [5], all of them mounting their transmission X-ray sources far from the specimen to be analyzed. Little different, but always with the X-ray source far from the specimen were the attachments proposed by Eckert (both reflection [6] and transmission [7,8]) and Pozsgai (transmission mode, but with the analyzed specimen in a closed space, protected from unwanted X-rays [9]). Other works, dealing with analogous SEM attachments, are nicely described in a review article by Pozsgai [10].

A somewhat different solution was proposed by Cazaux [11] and implemented first in a surface analysis instrument [12] and later in a scanning electron microscope [13]. It consists of a thin film anode in close contact with a thin film sample. The X-rays created within the anode under

* Corresponding author. Address: Department of Electronics, Technological and Educational Institute of Athens, 12210 Aegaleo, Greece. Tel.: +30 210 6533781; fax: +30 210 6511723.
E-mail address: vala@ee.teiath.gr (E.S. Valamontes).

0168-583X/$ - see front matter © 2007 Elsevier B.V. All rights reserved.
doi:10.1016/j.nimb.2007.03.089

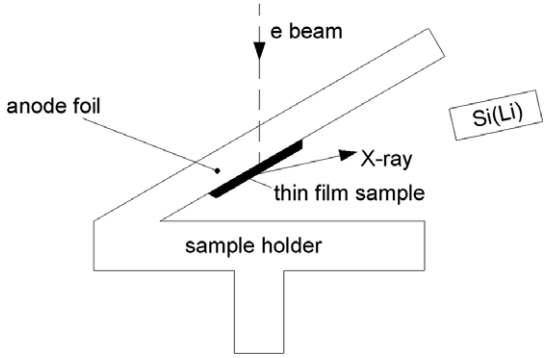

Fig. 1(a). Experimental setup used for back-foil XRF.

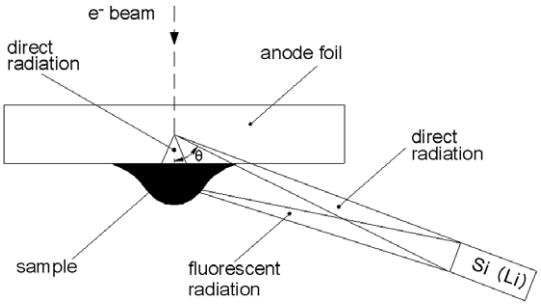

Fig. 1(b). Illustration of the trajectories of primary and fluorescence X-rays in back-foil XRF. The background is reduced by absorption of the continuous radiation, created by the electron beam, within the anode.

electron bombardment ionize the atoms of the sample. The corresponding SEM attachment is illustrated in Fig. 1. Compared to all the other proposed solutions, this experimental arrangement offers the ultimate resolution, which is in the μm range when the anode is sufficiently thin (of the order of the electron range). In this paper, this last solution is used (back-foil scanning X-ray microfluorescence) and the sensitivity of the technique for the analysis of very thin overlayers, where EPMA reaches its detection limits, is examined. Both experimental results and Monte-Carlo simulations are used in this respect. Direct comparison with EPMA is also made. The radial distribution of the obtained fluorescence signal is also calculated by Monte-Carlo simulations and experimental results.

2. Experimental setup

The experimental setup of Fig. 1(a) was used for back-foil XRF. The anode was composed of a silicon foil, 20 μm thick (case a) or a nickel foil, 5 μm thick (case b) or a silver foil, 5 μm thick (case c) or a gold foil, 2.5 μm thick (case d). The anode was chosen to be sufficiently thick so that primary beam electrons ($E_0 = 30$ keV) were prevented from reaching the Al film (cases a, c, d) or the Ti film (case b) on the back side of the anode. On the other hand, a limited thickness is necessary in order to minimize self absorption of the generated X-rays. Al films (cases a, c, d) or Ti films (case b) of different thicknesses (from 1 nm to 200 nm) were deposited on one side of the anodes by electron beam evaporation in high vacuum (10^{-3} Pa operating pressure). For the experimental calculation of the lateral resolution of scanning X-ray microfluorescence, we fabricate a pattern consisted of 10 μm Al lines and 10 μm spaces on the backside of Au and Si anodes. The thickness of Al lines is 200 nm.

A Si(Li) detector and an EDAX system for quantitative analysis were used for X-ray signal acquisition. The X-ray signal, integrated under the peak and the integrated background, also under the peak and in the same energy window, were used. Fig. 1(b) illustrates the trajectory of the direct and fluorescence X-rays in back-foil XRF. The background is reduced by absorption of the continuous radiation, created by the electron beam, within the anode. Standard EPMA, using the same experimental conditions of beam current and electron beam focusing was applied to the same samples.

3. Monte-Carlo calculations

The basic computational model for the calculation of electron trajectories was described in detail elsewhere [14]. It is based on the following assumptions:

- Elastic scattering is described by a screened Rutherford cross-section.
- Angle deviation is considered to be only due to elastic scattering, this is a good approximation, as inelastic scattering occurs through very small angles.
- Between two scattering points, electrons are considered to lose energy continuously. The energy loss is described by the Bethe equation [15] for energies $E > 6.4J$, where J is the mean ionization potential. For lower energies, the Rao-Sahib and Wittry's [16] expression is used.
- Each step length for elastic scattering is considered to be constant and equal to 1/100 of the total electron range (plural scattering model). The total length of the electron trajectory within the sample is taken to be the Bethe range. With this approximation, the calculation time is reduced significantly while little error is introduced. In order to evaluate the X-ray signal induced by electrons, each step is divided into smaller steps. At each small step, the energy and position of the electron is known, so the probability for X-ray generation is given by the corresponding cross-section.
- The X-ray emission is considered to be isotropic, two random numbers are used for the direction of X-ray emission. Some of these X-rays enter into the film after possible absorption within the anode.
- The X-ray fluorescence signal is calculated by dividing the film into 10 layers and considering the probability that the primary X-rays entering the layer are absorbed by the layer on their way out of the film. Absorption correction of the fluorescent X-ray signal created within the film is also considered. The absorption coefficients used are taken from the X-ray cross-section compilation by the Kaman Science Corporation [17].

4. Results and discussion

Fig. 2 indicates the experimental results of the signal to background ratio (S/B) in the case of back-foil XRF for different film thicknesses as a function of the detection angle θ. The acquisition time of the whole spectrum was equal to 600 s. When the angle is increased, the S/B ratio is improved, due to further reduction of the background caused by greater absorption of continuous radiation within the anode.

Fig. 3 shows the ratio of the analyzed Al X-ray signal from the film to the Au signal from the anode. Points correspond to experimental results and full lines to Monte-Carlo calculations. Good agreement is observed between experiment and calculations. The Al signal from the films are increased with respect to the signals from the anodes as the detection angle θ is increased. This is due to the absorption. The absorption of the Au X-ray line from the anode is greater than the absorption of Al XRF signal from the films with the increase of θ angle.

EPMA was performed on the same samples for comparison. Fig. 4 illustrates experimental results of the signal to background ratio (S/B) for Al/Au system and three different angles of incidence. The signal from a thin film in EPMA is improved at low primary beam energies and high angles of incidence. However, the X-ray signal in back-foil X-ray microfluorescence and in electron probe X-ray microanalysis is of the same order of magnitude (in the case of very thin overlayers). In the first technique the background is reduced by absorption of the continuous radiation within the anode and it is significantly lower compared to the second one.

The same acquisition time was used for both EPMA and back-foil XRF spectra (600 s). The minimum detectable concentration (or thickness) is calculated by considering the Rose criterion, according to which a signal is detectable

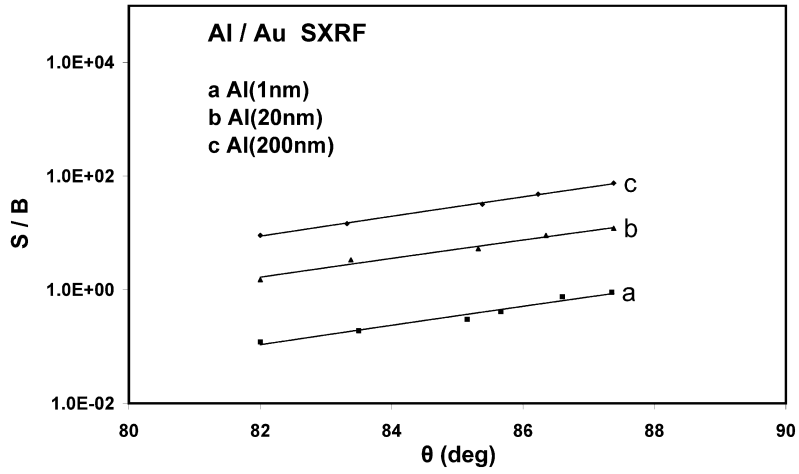

Fig. 2. Experimental values of the signal to background ratio (S/B) in the case of back-foil XRF for Al/Au system and different film thicknesses as a function of the detection angle θ.

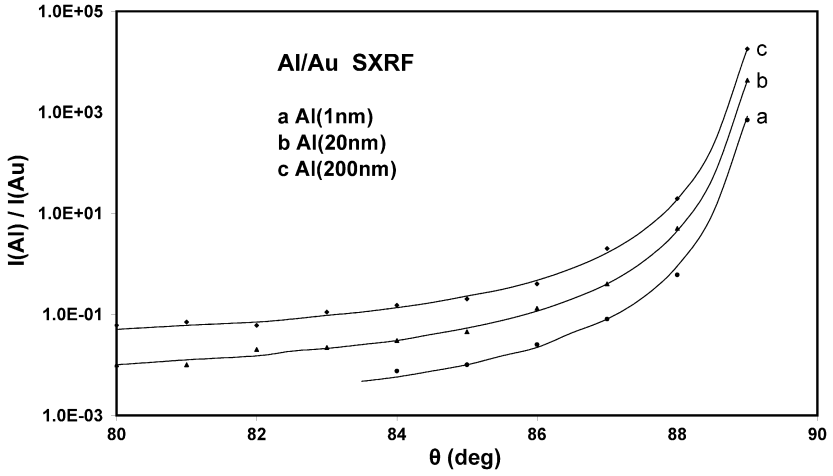

Fig. 3. Ratio of the Al X-ray signal from the film to the Au X-ray signal from the anode. Points correspond to experimental results and full lines to Monte-Carlo calculations.

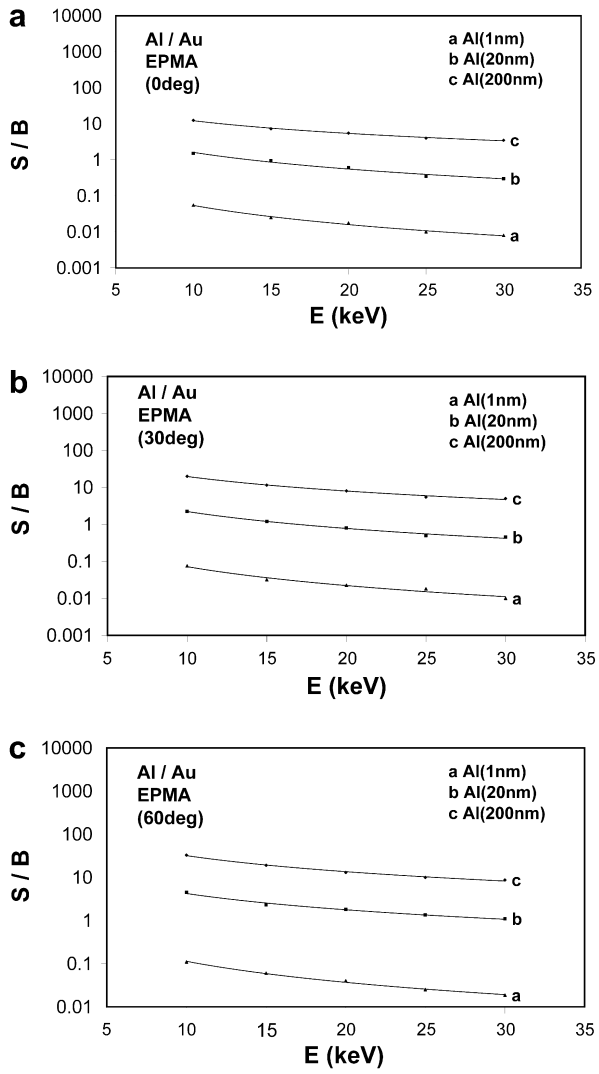

Fig. 4. ((a)–(c)) Experimental values (EPMA) of the signal to background ratio (S/B) for Al/Au system and three different angles of incidence (0°, 30°, 60°).

if the corresponding peak is at least three times the standard deviation of the background. By taking that into account the minimum detectable concentration X_m of an element A in a matrix may be expressed as

$$X_m = \frac{3}{I_S}\sqrt{\frac{I_{BG}}{t}},$$

where I_S is the signal from a standard containing only the element A and I_{BG} is the signal under the background. From the above expression it is obvious that the minimum detectable concentration is reduced if I_{BG} is smaller and the acquisition time is increased. In the case of back-foil XRF the reduced background gives the possibility to increase the measuring time so that the sensitivity of the technique is considerably improved compared to that of EPMA. Back-foil X-ray microfluorescence has very good relative detection limits between 10 and 500 ppm by weight range (in the case of very thin overlayers). The absolute detection limits are between 10^{-11} and 10^{-14} g. The detection limits of this technique depend strongly on the operating conditions. In contrast to SXRF, EPMA has relative detection limits of the order of magnitude of 0.1 wt.% (or 1000 ppm by weight).

The lateral distributions of the total X-ray signals from the films in back-foil XRF is given in Fig. 5 for primary beam energy of 30 keV (Monte-Carlo calculations). These distributions are approximately Gaussians. By applying the Rayleigh criterion as in reference [18,19], the lateral resolution of the technique, defined as the minimum distance between two points for which the X-ray signals are resolved, is calculated. Values of some micrometers are found for any SXRF system (Fig. 6). These lateral resolutions are by some orders of magnitude better than in standard XRF.

Fig. 7(a) and (b) indicate the line scan X-ray signal in the case of back-foil SXRF for Al/Au system (case a) and Al/Si system (case b). There is a pattern consists of 10 μm Al lines and 10 μm spaces on the backside of Au and Si anodes. The thickness of Al lines is 200 nm. The lateral resolution of scanning X-ray microfluorescence is of the order of one micrometer (case a) and of the order of ten micrometers (case b). The agreement between experimental results and Monte-Carlo calculations is very good.

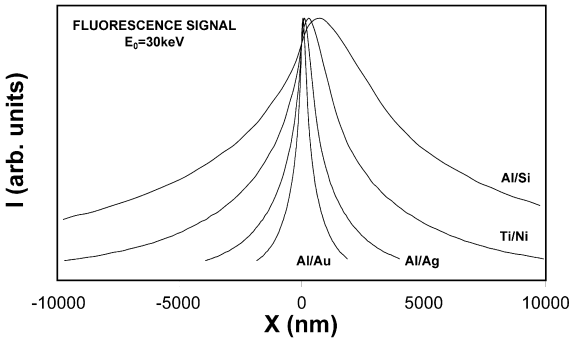

Fig. 5. The lateral distribution of the total X-ray signal from various back-foil XRF systems for primary beam energy of 30 keV and films thickness 200 nm.

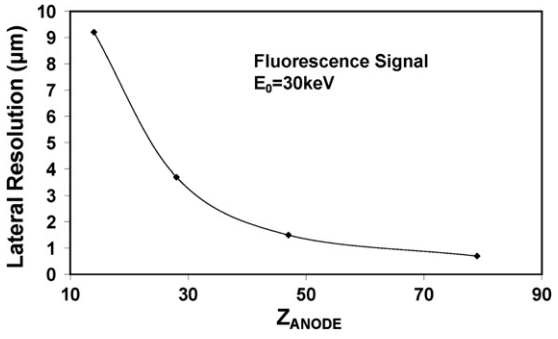

Fig. 6. The lateral resolutions of the technique for various systems, as a function of the atomic number of the anode (Monte-Carlo calculations). The primary beam energy is 30 keV and the films thickness is 200 nm. These lateral resolutions are by some orders of magnitude better than in standard XRF.

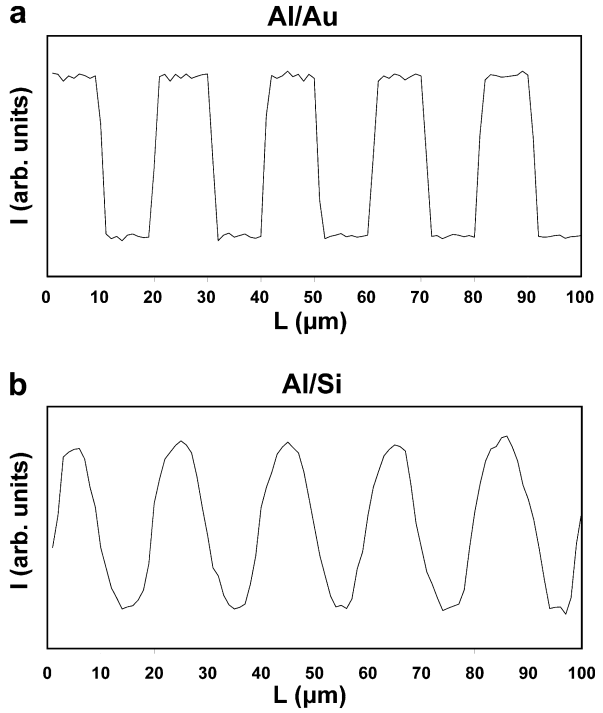

Fig. 7. (a) and (b) Line scan X-ray signal in the case of back-foil SXRF for Al/Au system (case a) and Al/Si system (case b). There is a pattern consists of 10 μm Al lines and 10 μm spaces on the backside of Au and Si anodes. The thickness of Al lines is 200 nm.

5. Conclusion

Back-foil scanning XRF and EPMA are both applied to the analysis of very thin films. The sensitivity of back-foil XRF is better than that of EPMA in the case of very small film thicknesses (up to a few tens of nm) for any SXRF system. The lateral resolution of back-foil XRF is of the order of some micrometers. This is much better than the lateral resolution in conventional XRF and of the same order of magnitude as in EPMA.

Further developments of this technique are:

(i) The chemical determination of thin films (e.g. insulators without depositing a conducting layer on the top of them and beam sensitive biological samples where these are not sensitive to the level of X-radiation involved) by point microfluorescence analysis.

(ii) Scanning X-ray radiography could be performed in an unmodified scanning electron microscope. The lateral resolution could be improved by a suitable choice of operating conditions, down to a few tenths of a micrometer.

(iii) The radiography of a wet specimen set, in the atmosphere, close to the foil target acting as a window.

Such a technique is not intended to compete with related techniques especially as regards the detection limits and the limits of the resolution. Our purpose is to offer new possibilities to the experimentalist for the analysis of thin films.

Acknowledgements

This work is co-funded by 75% from E.E. and 25% from the Greek Government under the framework of the Education and initial Vocational Training Program – Archimedes (project TEI of Athens 2.2 – 23).

References

[1] L.M. Middleman, J.D. Geller, in: Scanning Electron Microscopy, Chicago, 1976, p. 171.
[2] B. Linnemann, L. Reimer, Scanning 1 (1978) 109.
[3] M. Wendt, Patentschrift DD-WP139, 1978, p. 304.
[4] M. Wendt, T. Krajewski, in: Proceedings of 5 Tagung Microsonde, Physikalische der DDR, Leipzig, 1981, p. 125.
[5] R.M. Weiss, Beitr. Elektronenmikroskop. Direktabl. Oberfi. 2 (1979) 209.
[6] R. Eckert, in: Scanning Electron Microscopy, Chicago, 1983, p. 1535.
[7] W. Plannet, Leaflet Rontgenbox, Plano, Marburg, 1983.
[8] R. Eckert, Scanning 8 (1986) 232.
[9] I. Pozsgai, Inst. Phys. Conf. Ser. 78 (1985) 201.
[10] I. Pozsgai, X-ray Spectrom. 20 (1991) 215.
[11] J. Cazaux, Rev. Phys. Appl. 10 (1975) 263.
[12] D. Mouze, X. Thomas, J. Cazaux, in: J.D. Brown, R.H. Packwood (Eds.), Proceedings of the 11th International Congress on X-ray Optics and Microanalysis, London, Canada, 1986, p. 63.
[13] E. Valamontes, A.G. Nassiopoulos, in: Proceedings of the III Balkan Congress on Electron Microscopy, Athens, 1989, p. 267.
[14] A.G. Nassiopoulos, E. Valamontes, Surf. Interface Anal. 15 (1990) 405.
[15] H. Bethe, Ann. Phys.-Leipzig 5 (1930) 325.
[16] T.S. Rao-Sahib, D.B. Wittry, J. Appl. Phys. 45 (1974) 5060.
[17] X-ray Cross-section Compilations from 0.1 keV to 1 MeV, Kaman Science Corporation, Colorado Springs, Colorado, 1985.
[18] E. Valamontes, A.G. Nassiopoulos, N. Glezos, Surf. Interface Anal. 19 (1992) 419.
[19] E.S. Valamontes, J.C. Statharas, Vacuum 77 (2005) 371.